Increased Innate Function Following HIV-1 Suppression Is Linked to Epigenetic Changes

Eileen P. Scully[1,2], Ainsley Lockhart[1], Wilfredo Garcia-Beltran[1], Christine D. Palmer[1], Chelsey Musante[1], Eric Rosenberg[3], Todd M. Allen[1], J Judy Chang[4], Ronald J. Bosch[5], Marcus Altfeld[1,6]

[1]Ragon Institute of MGH, MIT, and Harvard, Massachusetts General Hospital, Cambridge, MA, United States, [2]Division of Infectious Diseases, Brigham and Women's Hospital, Harvard Medical School, Boston, MA, United States [3]Division of Infectious Diseases, Massachusetts General Hospital, Boston, MA, United States, [4]University of Melbourne, Melbourne, Australia, [5]Harvard School of Public Health, Boston, MA, United States and [6]Heinrich-Pette-Institut, Leibniz Institute for Experimental Virology, Hamburg, Germany.

Background and Rationale

HIV-1 infection leads to both profound immune suppression and pathologic inflammation. While adaptive immune dysfunction has been extensively studied, less is known about innate immunity in the context of HIV-1. Based on the broad pathogen susceptibility in progressive HIV-1, we hypothesized that there would be aberrant innate responses. We tested innate function with ex vivo stimulation with a panel of innate agonists measuring bulk cytokine production and intracellular staining patterns. Changes in innate function were analyzed in relationship to plasma inflammatory markers and log viral load. We sought to determine molecular mechanisms of altered innate function, analyzing subset distribution, transcription factor translocation, and epigenetic modifications.

Methods

Patients population
Subjects from the Boston Acute HIV Cohort, (MGH) with PBMC and plasma samples available before and after initiation of antiretroviral therapy (ART) were selected (Table 1).

T cell activation
CD4⁺ and CD8⁺ T cells were assessed by flow cytometry for coexpression of CD38 and HLADR. CD4 count and HIV viral load were determined by standard clinical assays.

Stimulation
Thawed PBMCs were cultured with a panel of innate immune stimuli including LPS (TLR4), HKLM (TLR2), n-muramylglycopeptide (NOD), and curdlan (dectin-1) for 24 hours. Bulk cytokine production was assessed from culture supernatants by mulitplex luminex assay (GMCSF, CCL20, IFNγ, IL-10, IL-6, IL-1β, and TNFα). Paired cultures with addition of protein export inhibitor were stained for intracellular protein production (TNFα and IL-1β) and analyzed by flow cytometry.

Plasma cytokines and microbial translocation markers
Plasma samples matched to PBMCs were assessed for cytokines by mulitplex assay(IL-10, IL-6, IL-7, MCP-1, IP-10, IL-1β, IFNγ, IFNα2, MIP-1β, TNFα). CD163 (sCD163) and soluble CD14 (sCD14) were measured by ELISA and LPS was measured with the limulus amebocyte assay (LAL).

NFκB nuclear translocation
Cryopreserved PBMCs were thawed, rested and analyzed as either untreated or following a one hour LPS stimulation. Samples were stained with CD14, intracellular NFκB and DAPI (nuclear stain). Images were acquired of single, focused, DAPI⁺, CD14⁺ cells hierarchically gated on an Imagestream X Mark II. NFkB nuclear translocation was measured by Similarity Score, a log-transformed Pearson's correlation coefficient comparing pixel values of the DAPI and NFkB stains, IDEAS software (Amnis).

Chromatin Immunoprecipitation
Epigenetic modifications at the TNF-α promoter were assessed by (ChIP). Cryopreserved PBMCs were thawed from one viremic and one suppressed timepoint from each patient, and enriched for monocytes using an AutoMACS Monocyte Isolation Kit (Miltenyi). Equal numbers of monocytes from each patient were pooled into viremic and suppressed samples. ChIP was performed using a Magna ChIP HiSens Chromatin Immunoprecipitation Kit (Millipore) with antibodies to he following histone modifications H3K4me3, H3K9me1, H3K27me3, H4Ac, and IgG (Millipore). qPCR was performed using primers for four regions of the TNFα promoter that have been previously described. Enrichment was calculated by comparison of IP samples to input DNA and background IP was subtracted out based on enrichment of nonspecific IgG. Fold change in histone occupancy was calculated between viremic and suppressed samples.

Statistical analysis
Multivariate analysis of supernatant cytokine levels was done with partial least squares discriminant analysis separating samples into viremic and suppressed categories. Associations between innate responses and plasma factors were assessed using resampled Spearman correlations and generalized estimating equations to account for repeated sampling(Follmann et al., *Biometrics*, 2003). Multivariate analysis of plasma factors in relationship to the intracellular cytokine staining Comparisons in subset distribution were done with Mann Whitney nonparametric statistics.

Results

Table 1.

Table 1. Demographic and Clinical Characteristics of Study Subjects

Age in years, median (range)	36 (24-48)
Male gender (%)	100
Race/ethnicity (%)	
Black	25
White non-Hispanic	37.5
Hispanic	37.5
HIV-1 risk factor	MSM
Pretreatment viral load in copies/mL median(range)	86,950 (35,800-6,750,000)

Results

Figure 1:
Relationship of T cell activation and absolute CD4 count to declining viral load under ART

Figure 1. PBMCs from timepoints spanningthe period of viral suppression were analyzed for T cell activation based on CD38 and HLA-DR coexpression. **A.** Correlation between CD8⁺ T cell activation and declining viral load, p<0.001 and r=0.87. **B.** CD4 T cell activation and log viral load correlation p<0.001 and r=0.66. **C.** Correlation between absolute CD4 count determined by clinical testing and log viral load had a p<0.001 and -0.30. Colors indicate individuals resampled over time, all statistics corrected for resampling with a repeated measures model and X axis with highest viral load at the origin. **D.** Representative flow plots quantifying T cell activation with corresponding plasma viral loads from a single individual

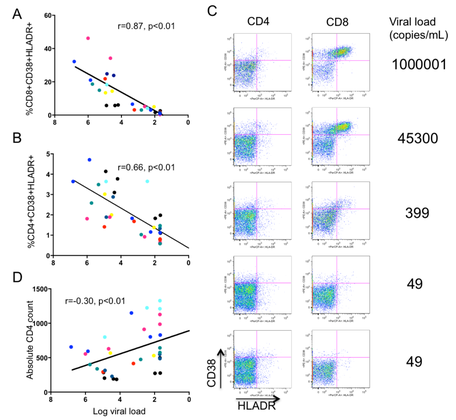
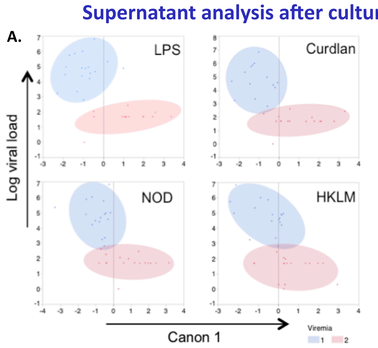


Figure 2:
Supernatant analysis after culture of bulk PBMCs with innate immune stimulants



B.

Stimulant	Cytokine	R value	P value
LPS	IL-1β	-0.36	<0.01
	CCL20	-0.41	0.01
	IL-10	-0.31	0.21
	TNFα	-0.37	<0.01
	GMCSF	-0.02	0.75
	IFNg	-0.23	0.02
	IL-6	-0.17	0.43
Curdlan	IL-1β	-0.52	<0.01
	CCL20	-0.52	<0.01
	TNFα	-0.45	<0.01
NOD	CCL20	-0.38	<0.01
	IL-6	-0.39	<0.01

Figure 2. Culture supernatants were analyzed by luminex for GMCSF, CCL20, IFNg, IL-10, IL-6, IL-1b, and TNFa after 24hours of stimulation. **A.** PLSDA was used to discriminate between samples derived from high viremia (1, blue) and viral suppression to <400 copies/mL (2, pink) (n=8 individuals with multiple timepoints for each individual). Models were able to classify the samples with a single canonical value (Canon-1, on the x-axis, unique for each stimulant). Model performance estimates predicted classification accuracy of 84% (LPS), 86%(Curdlan), and 85%(NOD) with lower performance for HKLM (71%) Over 10 iterations of the model with random exclusion of 10 data sets for validation., average predictive accuracy values were 87% (LPS), 88%(Curdlan), and 84%(NOD). HKLM had less consistent model performance, with 74% accuracy. **B.** Univariate relationships between cytokine production and viral load by Spearman analysis with repeated measures correction. No significant relationships were found for HKLM(TLR2).

Figure 3:
Intracellular cytokine staining after culture with innate immune stimulants.

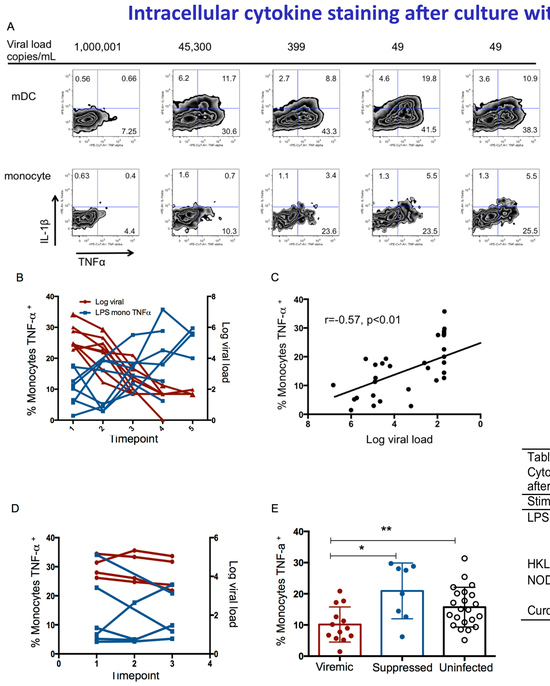


Figure 3. A. PBMCs were cultured with stimulants or media alone with addition of a protein export inhibitor at time zero. At harvest, cells were stained for surface markers to identify monocytes (CD3-/19-/56-/HLADR⁺CD14⁺) and mDCs (CD3-/19-/56-/HLADR⁺/CD14⁻/CD123⁻/CD11c⁺) producing IL-1β and/or TNFα. Representative staining from a single subject across a range of viral loads is shown in panel A. **B.** An inverse relationship between viral load and monocyte production of TNFα was identified. **C.** Overall correlation between log viral load and monocyte production of TNFα was significantly correlated with a r value of -0.57. **D.** No consistent change in cytokine production from individuals who were not initiated on ART was idenfitied. **E.** Cytokine production was significantly lower than uninfected subjects at the timepoint of highest viral load.

Table 3. Correlation of plasma log viral load to cytokine production. Cytokine production by specific cell types by intracellular cytokine staining after stimulation with an innate agonist.

Stimulant	Cell type and cytokine	R value	P value
LPS	monocyte TNF-α	-0.57	p<0.001
	mDC TNF-α	-0.54	p<0.001
	mDC IL-1β	-0.58	p<0.001
HKLM	monocyte IL-1β	-0.40	p=0.002
NOD	monocyte IL-1β	-0.45	p<0.001
	mDC IL-1β	-0.47	p<0.001
Curdlan	mDC IL-1β	-0.28	p<0.001

Figure 4:
Multivariate modeling of the relationship between monocyte TNFα production and plasma factors

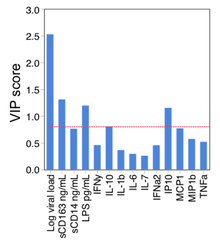


Figure 4. Multiple plasma factors were measured and partial least squares regression was used to build a model to predict the monocyte TNFα production in response to LPS stimulation. The variable importance in projection score was highest for log viral load If this measure was not included, the remaining variables could not be used to build a predictive model.

Figure 5:
Investigating the underlying determinants of altered monocyte function.

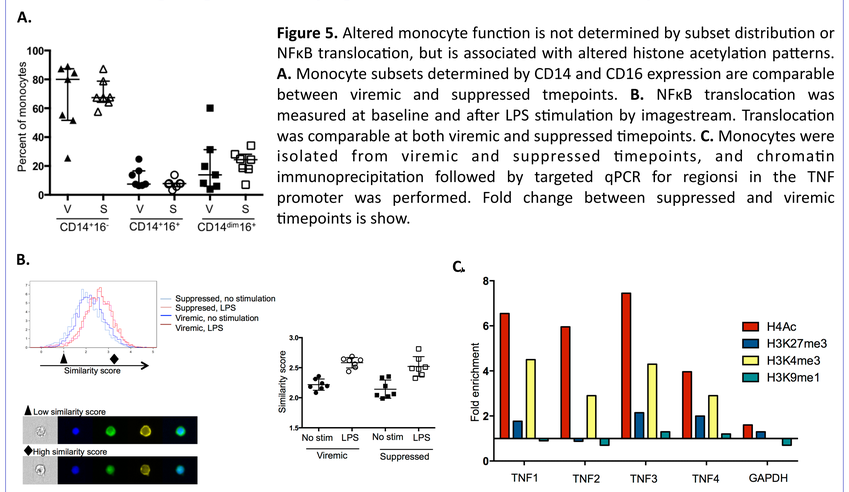
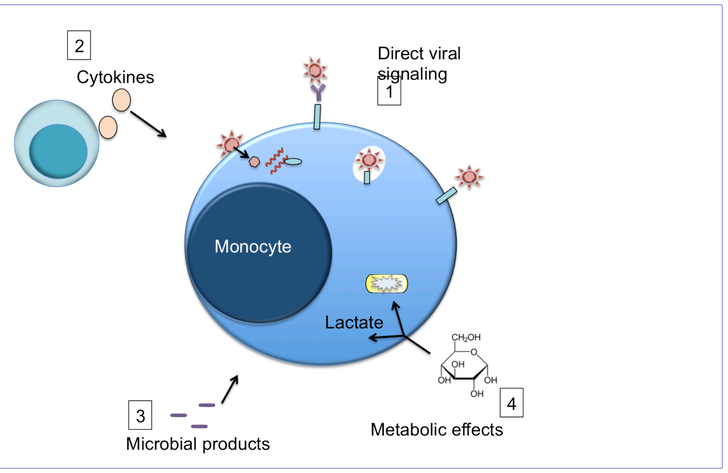


Figure 5. Altered monocyte function is not determined by subset distribution or NFκB translocation, but is associated with altered histone acetylation patterns. **A.** Monocyte subsets determined by CD14 and CD16 expression are comparable between viremic and suppressed tmepoints. **B.** NFκB translocation was measured at baseline and after LPS stimulation by imagestream. Translocation was comparable at both viremic and suppressed timepoints. **C.** Monocytes were isolated from viremic and suppressed timepoints, and chromatin immunoprecipitation followed by targeted qPCR for regionsi in the TNF promoter was performed. Fold change between suppressed and viremic timepoints is show.



Conclusions

Suppression of HIV-1 viral load with ART correlated with increased *ex vivo* innate immune responses. The altered monocyte function was not associated with subset redistribution or changes in NFκB signaling, but was associated with epigenetic modifications at the TNFα promoter. The high viral load environment conditions an epigenetic program associated with decreased innate function that is reversed with virus suppression. Further work is warranted to elucidate additional epigenetic determinants of innate immune deficiency and excessive inflammation in HIV-1 infection and their functional recovery following viral control.

Acknowledgements

Work was supported by a T32 AI007387 to EPS and R01 AI 078784 (MA PI) and the Ragon Institute Innate Immunity program (MA PI). We are grateful to Ragon Institute clinical and flow cytometry core and to the study subjects.